STUDY OF SOLAR CORONAL MASS EJECTIONS IN SPHERICAL GEOMETRY

Piyali Chatterjee
Indian Institute of Astrophysics
Bangalore

Pencil-code user meeting, 27-31 Jul, 2020, Glasgow

INDIA'S FIRST SOLAR MISSION: ADITYA-L1

Payloads: 7 nos

REMOTE instruments-4 nos

a. Visible Emission Line Coronagraph (VELC):
Continuum channel (1.05-1.5 Rs),
Spectrograph (coronal red/green lines),
spectropolarimetry (NIR Fe line, magnetic field measurements)

b. Solar Ultraviolet Imaging Telescope (SUIT):
Full disk (200-400 nm) Study of prominences, solar irradiance

IN-SITU instruments-3 nos

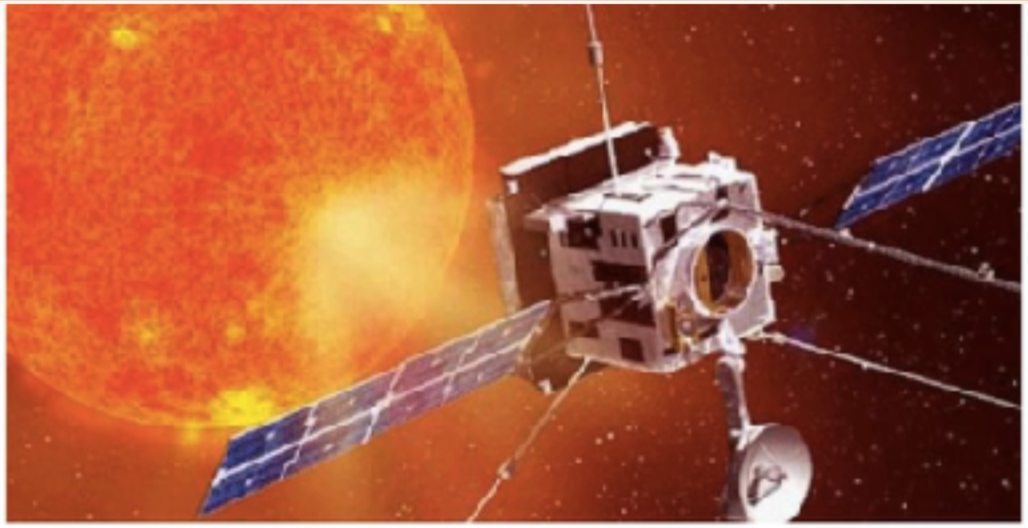

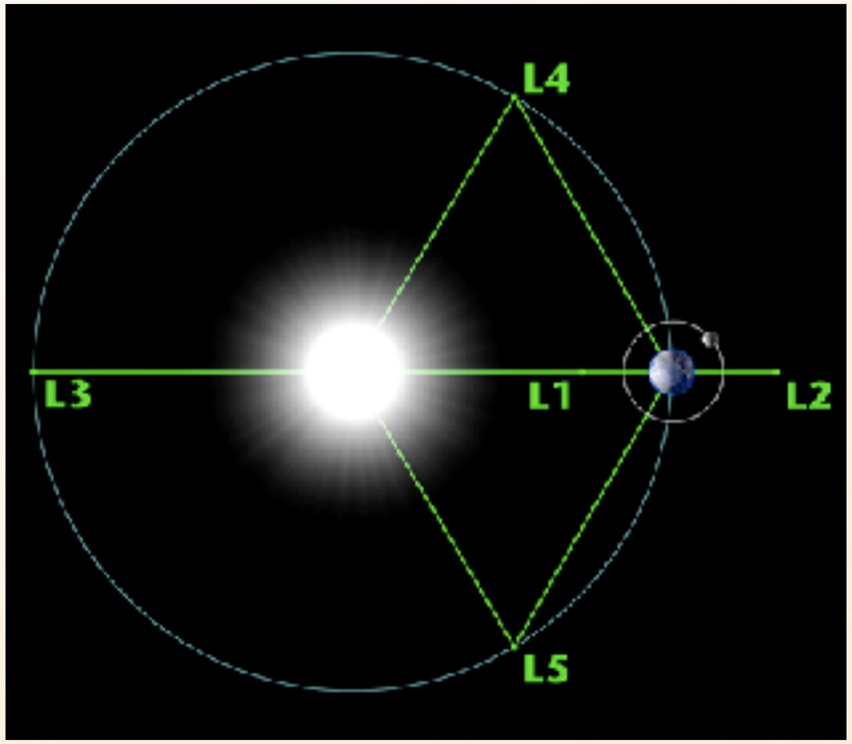

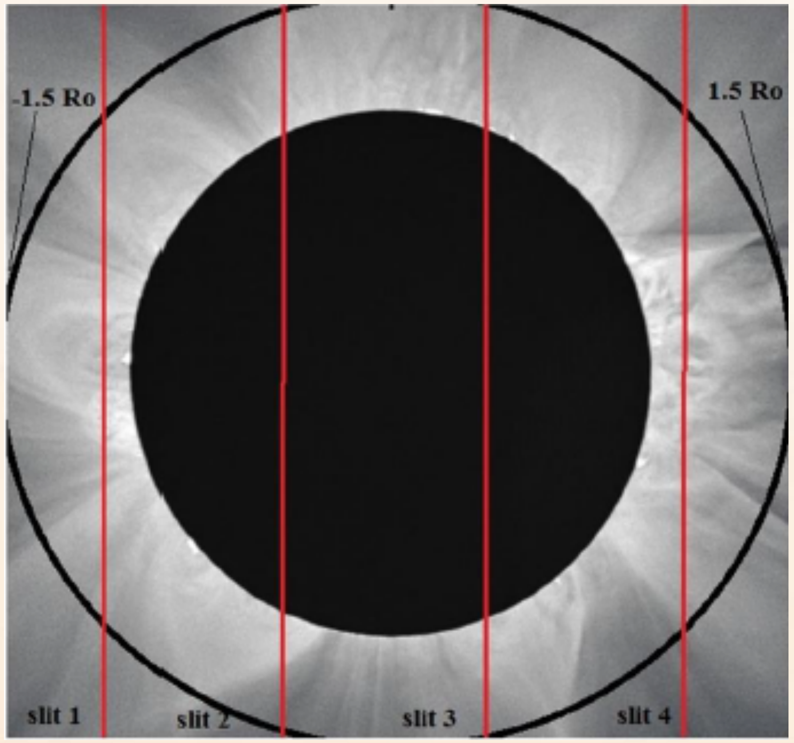

CME: 3-part structure

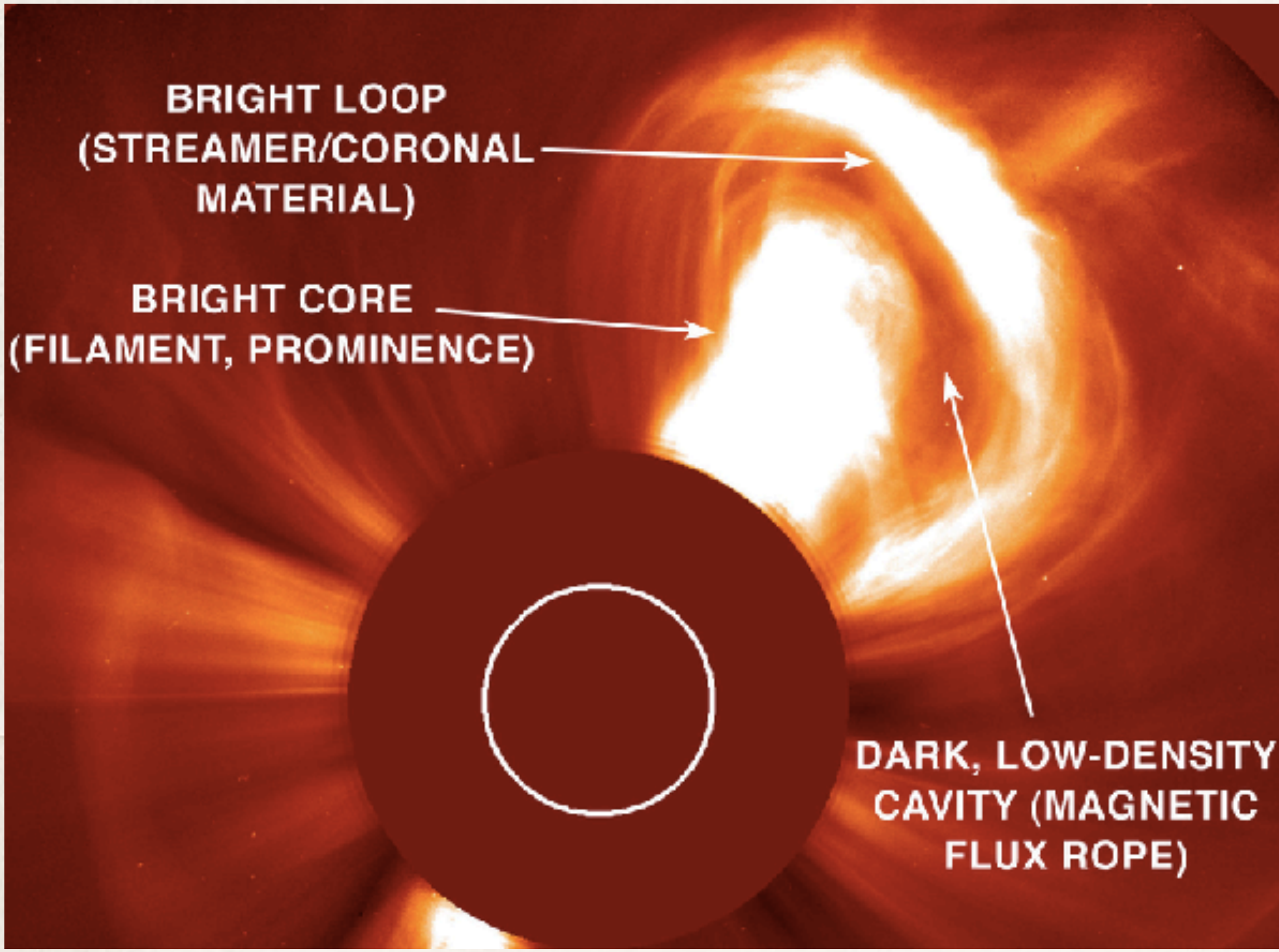

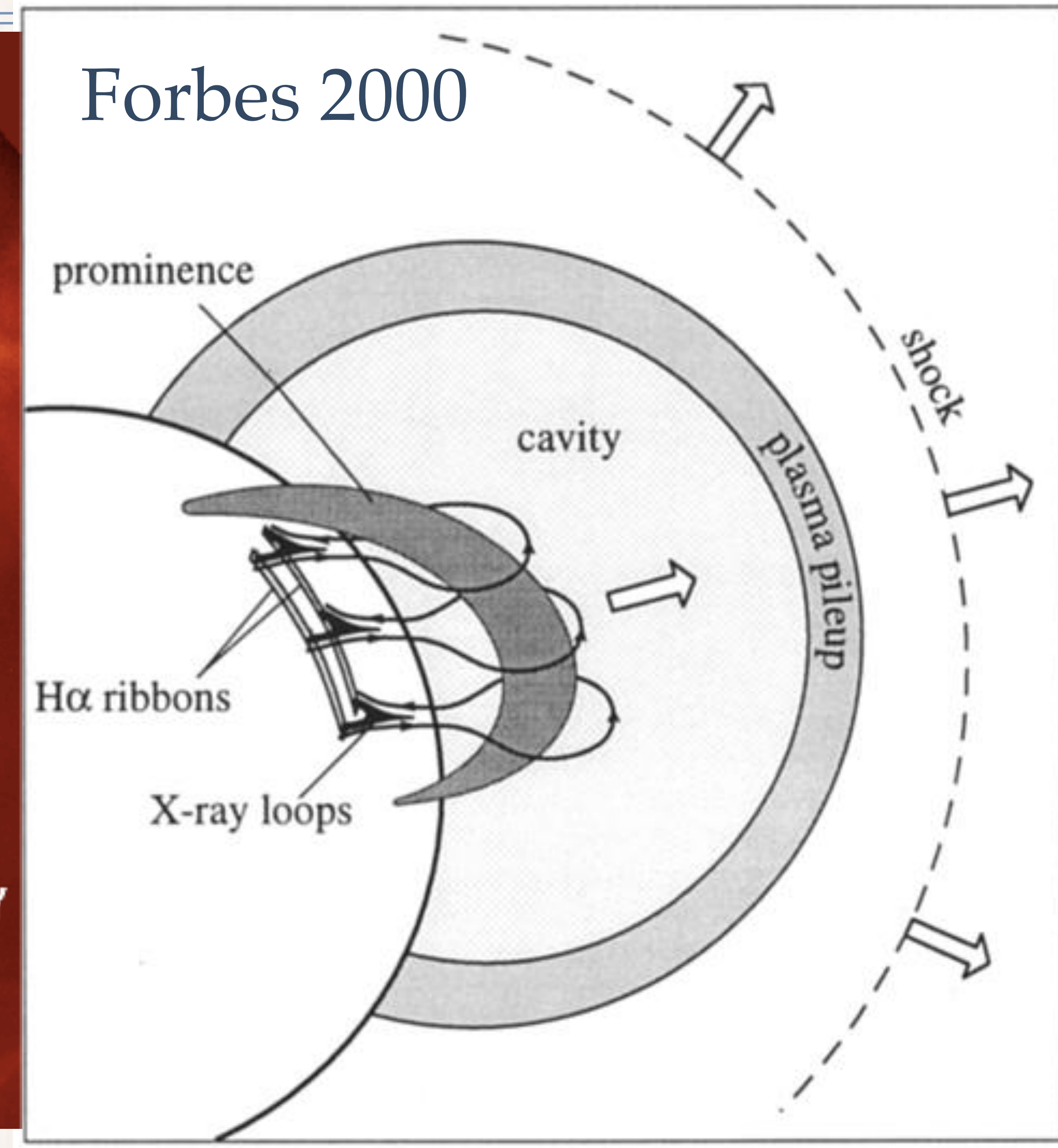

Considered standard morphology. Although only 30% of observed CMEs show all three parts! (*Webb & Hundhausen 1987*)

CME precursor: Flux rope formation

The magnetic flux rope (MFR) fits beautifully into the 3-part structure of the CME (Filament-Cavity-Frontal loop).

How does a flux rope form?

1. Shearing of foot points and Flux cancellation

2. Emergence of a twisted flux rope

CME precursor: Flux rope formation

1. Shearing and Flux cancellation [Chatterjee et. al. 2016]

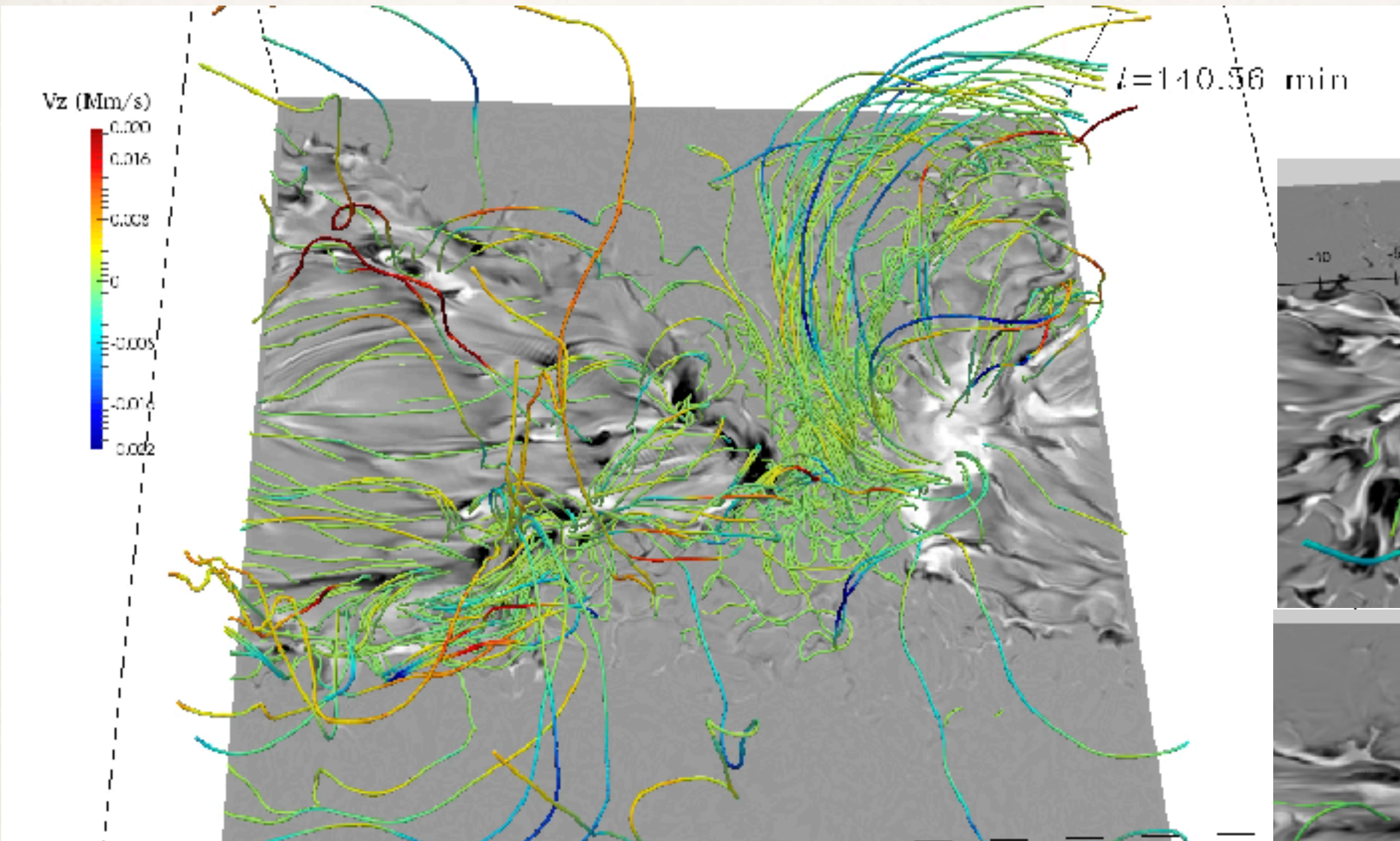

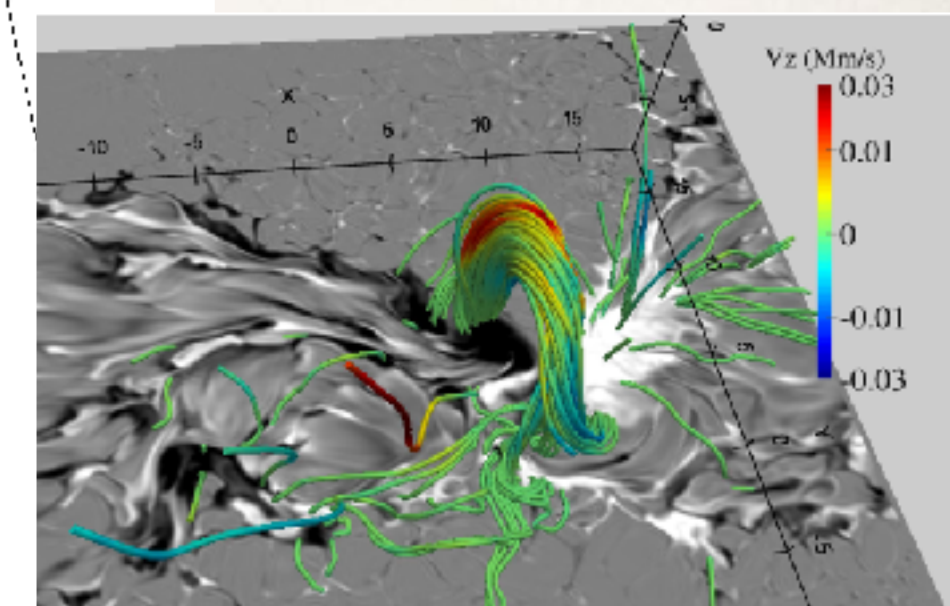

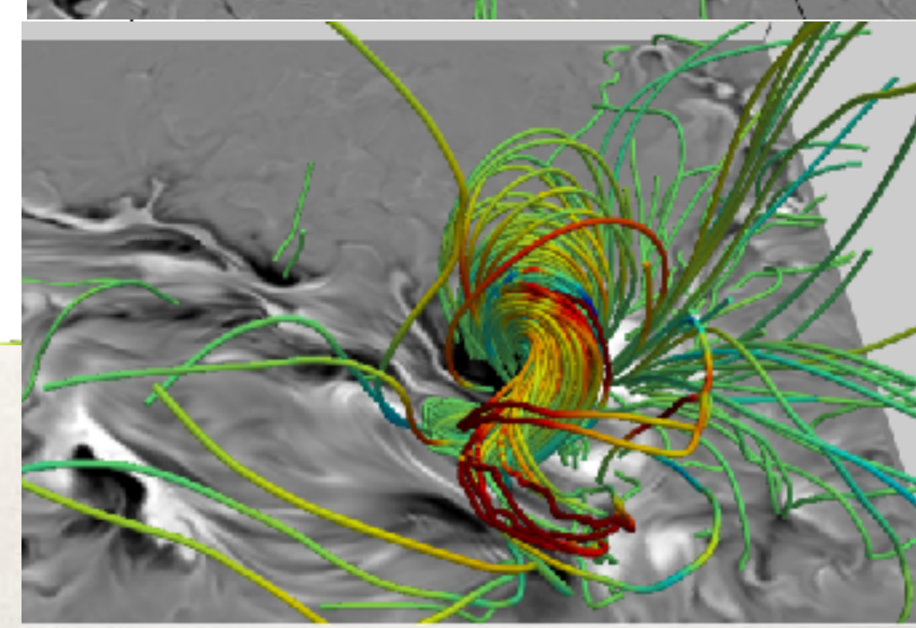

My typical (data inspired) CME initiation model

$$v_{z0} = 1.8\,\mathrm{km\,s^{-1}}$$

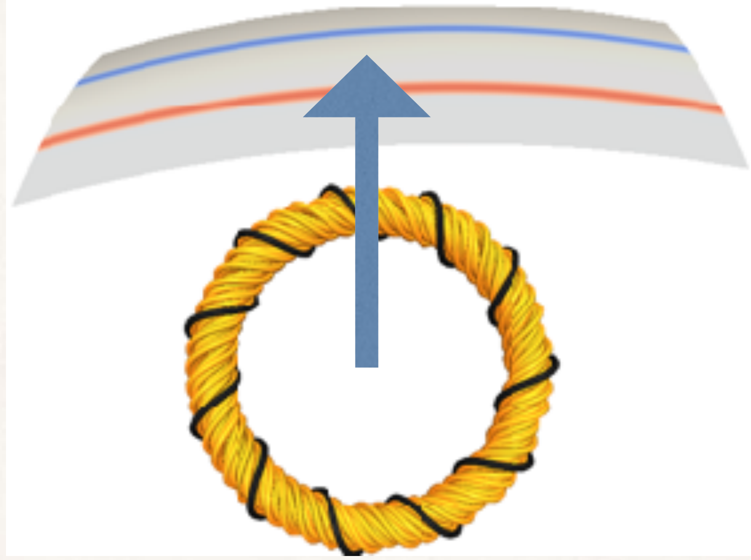

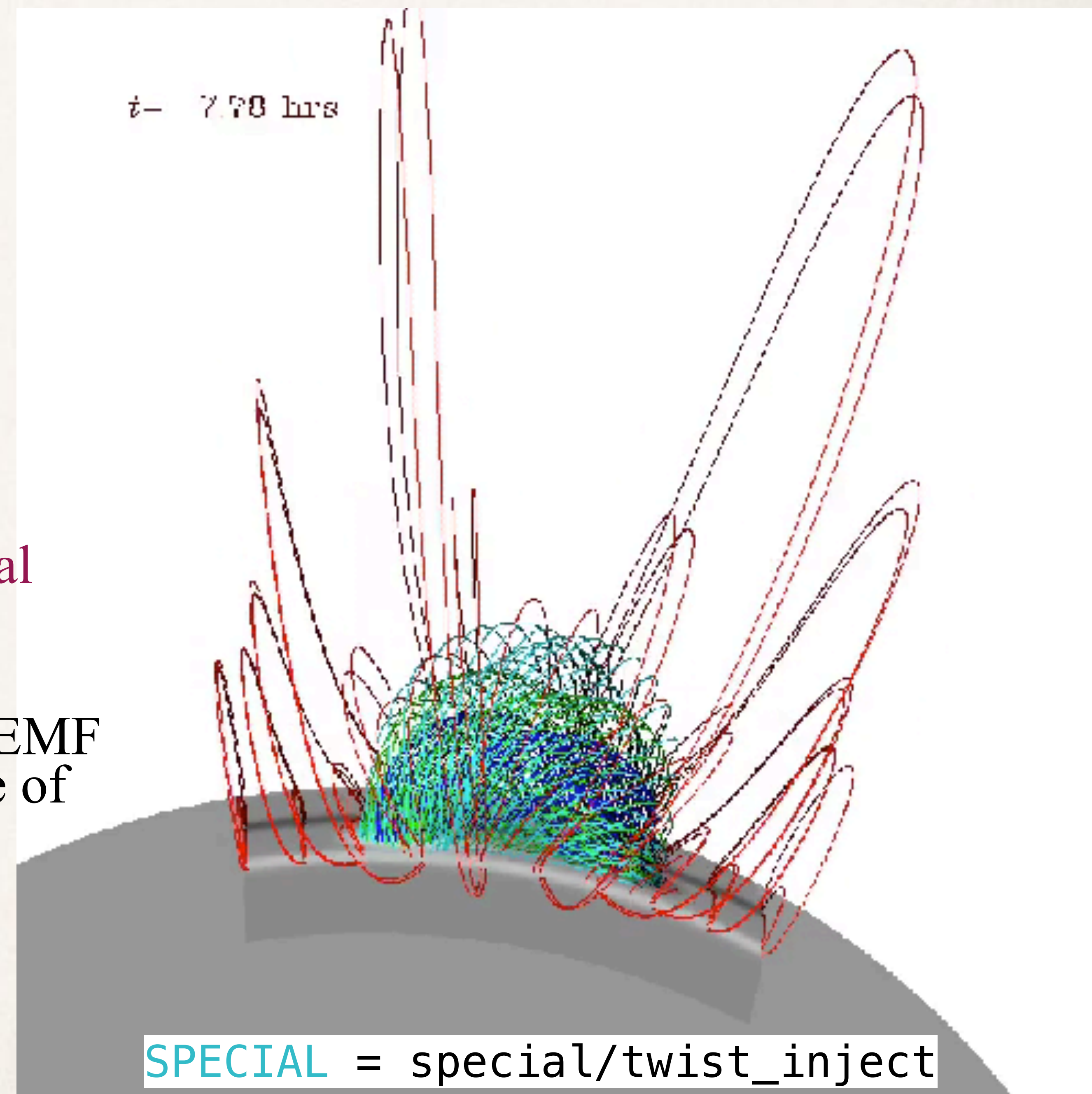

- 512X128X192 uniform/non-uniform grid, Initial isothermal stratified atmosphere at 1MK

- Forced kinematically at lower boundary by an EMF (= **v**×**B**) corresponding to **sustained** emergence of **twisted** torus into an ambient arcade

- Arcade field at lower boundary: 20G; Flux rope axis: 50 G
- **Thermal conduction along field lines**
- **Semi relativistic Boris correction (Boris 1970)**

CMEs under helmet streamers

Use of arcade magnetic field is
inspired by observations of CMEs forming under
helmet streamers

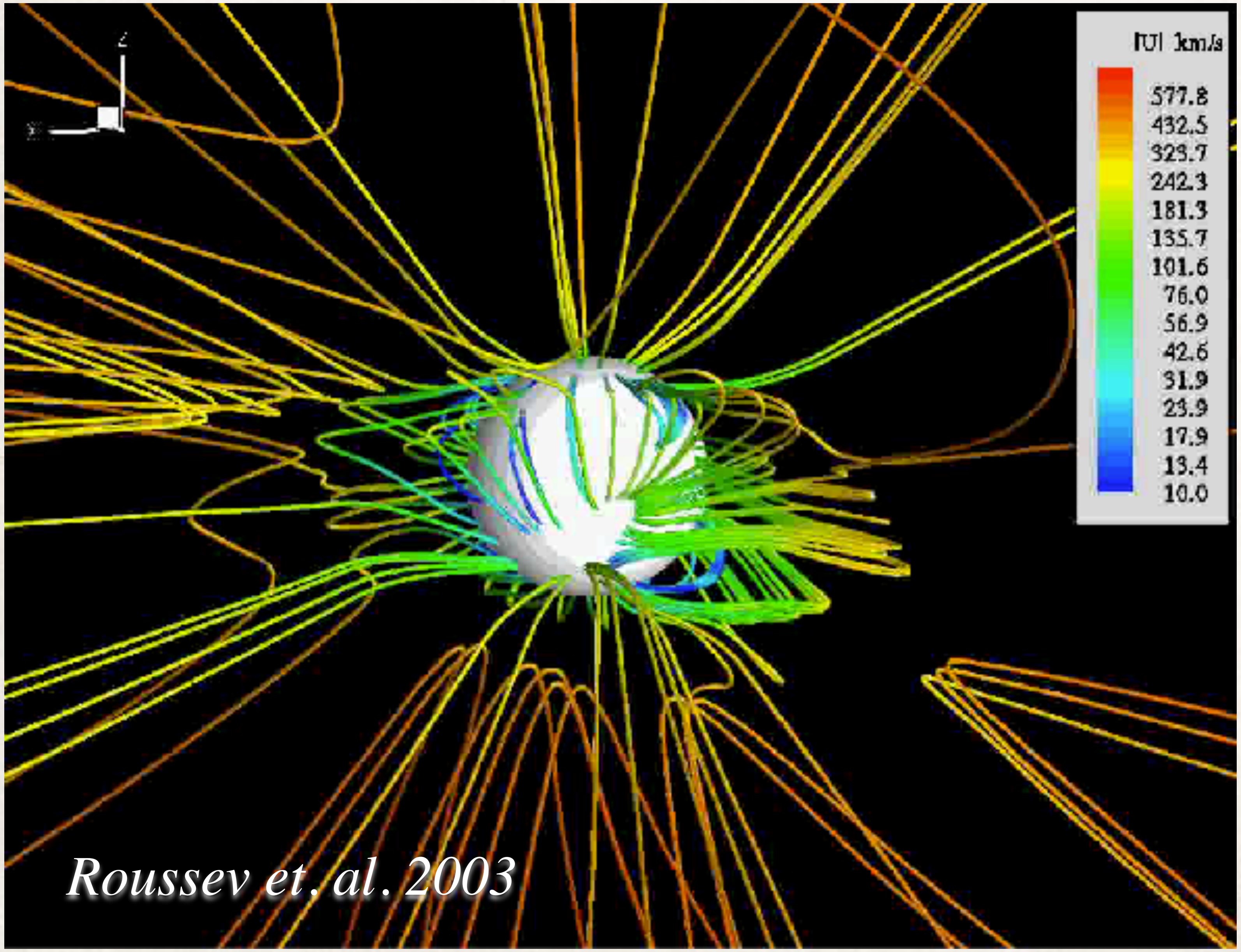

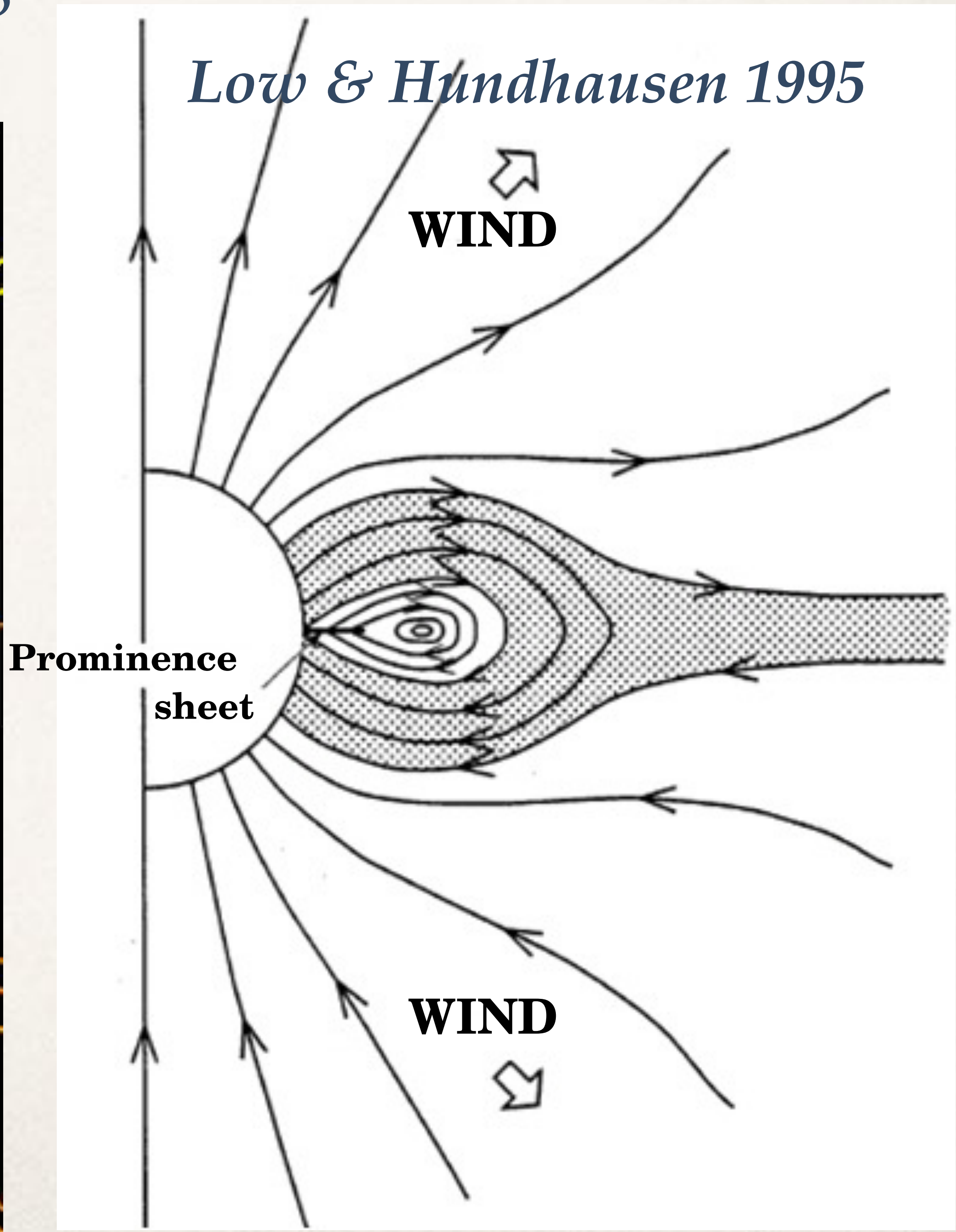

Compressible MHD equations

Mass conservation $$\frac{D\ln\rho}{Dt} = -\vec{\nabla} U$$

Navier-Stokes with semi-relativistic correction $$\frac{DU}{Dt} = -\frac{\vec{\nabla} p}{\rho} + g_z\hat{\vec{z}} + \frac{J\times B}{\rho} + \vec{F}_L^{\mathrm{corr}} + \rho^{-1}\mathbf{F}_{\mathrm{visc}}\,,$$

Induction $$\frac{\partial A}{\partial t} = U\times B - \eta\mu_0 J$$

Temperature

```
ENTROPY   =   temperature_idealgas
```

$$\rho c_V T\frac{D\ln T}{Dt} = -(\gamma-1)\rho c_v T\vec{\nabla}U + \vec{\nabla}\cdot\vec{q}_{\mathrm{cond}} + \vec{\nabla}\cdot(\rho T\chi_t\vec{\nabla}\ln T)$$
$$+\eta\mu_0 J^2 + 2\rho\nu\mathbf{S}_{ij}^2 + \rho\zeta_{\mathrm{shock}}\,(\nabla\cdot U)^2 - \rho^2\Lambda(T)$$

Field aligned Spitzer conductivity

```
HEATFLUX   =   heatflux
```

$$\vec{q}_{\mathrm{cond}} = K_{\mathrm{sp}}T^{5/2}\hat{b}(\hat{b}\cdot\nabla T)\,,$$

ASIDE ON BORIS CORRECTION

The need for having a semi-relativistic correction to the Lorentz force term in the velocity equation comes from the fact that in non-relativistic plasmas, the Alfven velocity can become comparable to the speed of light, c. Non-trivial displacement current. Circumvents the time step constraint due to large Alfven speed.

Gombosi et. al. 2002

$$\left[\mathbf{I}+\frac{v_A^2}{c^2}\left(\mathbf{I}-\hat{\boldsymbol{b}}\hat{\boldsymbol{b}}\right)\right]\cdot\frac{\partial \boldsymbol{U}}{\partial t} = -(\boldsymbol{U}\cdot\boldsymbol{\nabla})\boldsymbol{U}-\frac{\boldsymbol{\nabla}p}{\rho}+g_z\hat{\boldsymbol{z}} + \left[\frac{(\boldsymbol{\nabla}\times\boldsymbol{B})}{\mu_0\rho}+\frac{(\boldsymbol{\nabla}\times\boldsymbol{E})\times\boldsymbol{U}}{\mu_0\rho c^2}\right]\times\boldsymbol{B}\,.$$

Enhanced inertia matrix

```
&magnetic_run_pars
  lweyl_gauge=T
  lbb_as_aux=F
  lboris_correction=T,
  cmin=5.0 ! [5.0 Mm/s]
 /
```

$$F_L^{\mathrm{corr}} = \frac{\beta_A^2}{1+\beta_A^2}\left[\mathbf{I}-\frac{\hat{\boldsymbol{b}}\hat{\boldsymbol{b}}}{1+\beta_A^2}\right]\left[\boldsymbol{U}\cdot\boldsymbol{\nabla}\boldsymbol{U}+\frac{\boldsymbol{\nabla}p}{\rho}-g_z\hat{\boldsymbol{z}}-\frac{(\boldsymbol{\nabla}\times\boldsymbol{B})\times\boldsymbol{B}}{\mu_0\rho}\right].$$

```
p%clight2=spread(max(cmin**2,25*maxval(p%u2),maxval(p%cs2)),1,nx)
```

Chatterjee, 2019, GAFD, Pencil code special issue

Storage and release model of CMEs

Slow Emergence of a *twisted* flux rope similar to continually heating a pressure cooker

Valve modelled by ambient coronal magnetic field

Vapor pressure of steam build up of magnetic helicity in corona

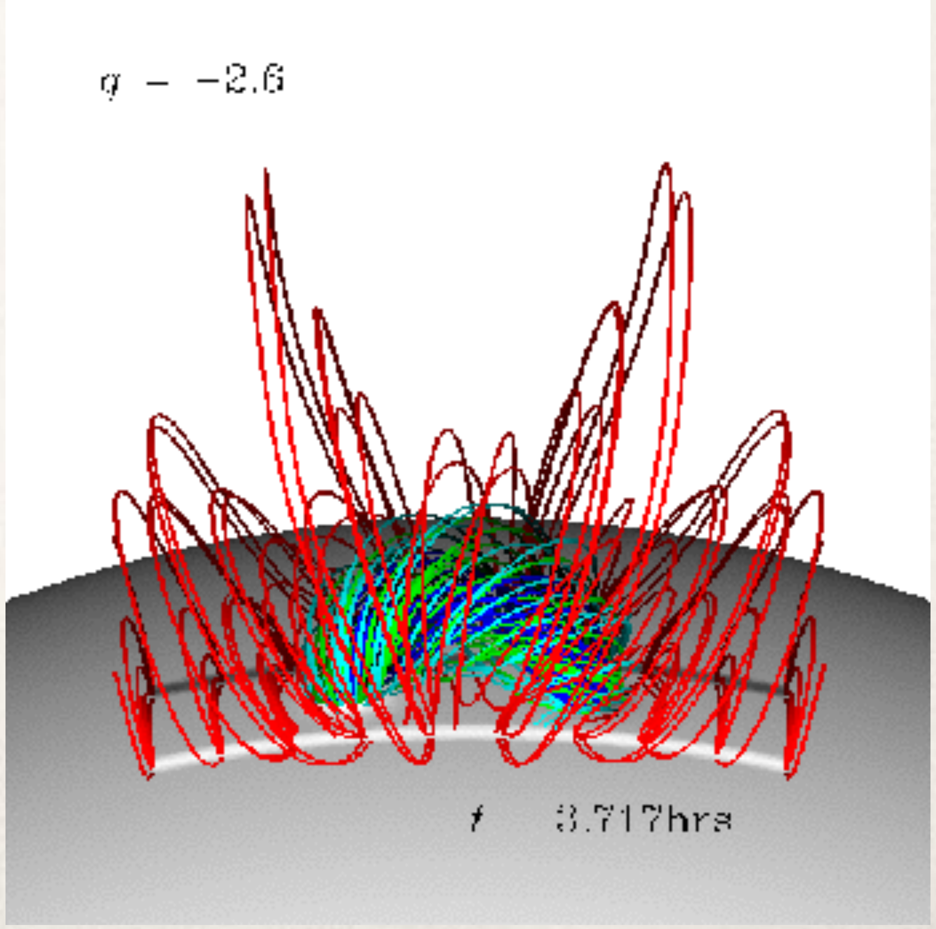

Tether cutting and formation of soft X-ray sigmoid

Slow Build-up phase

Hot current channel forms and field lines passing through the hot channel are sigmoidal in shape and show up in soft X-rays

Hinode

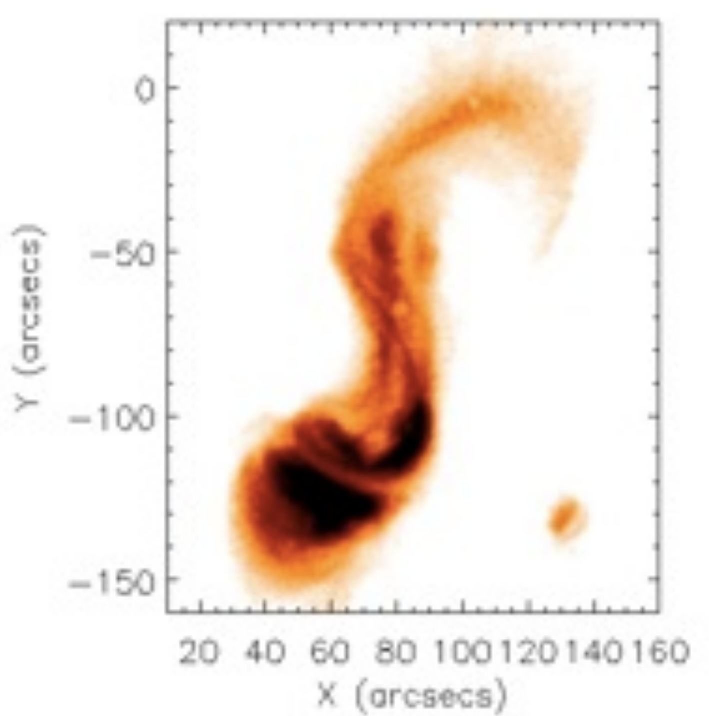

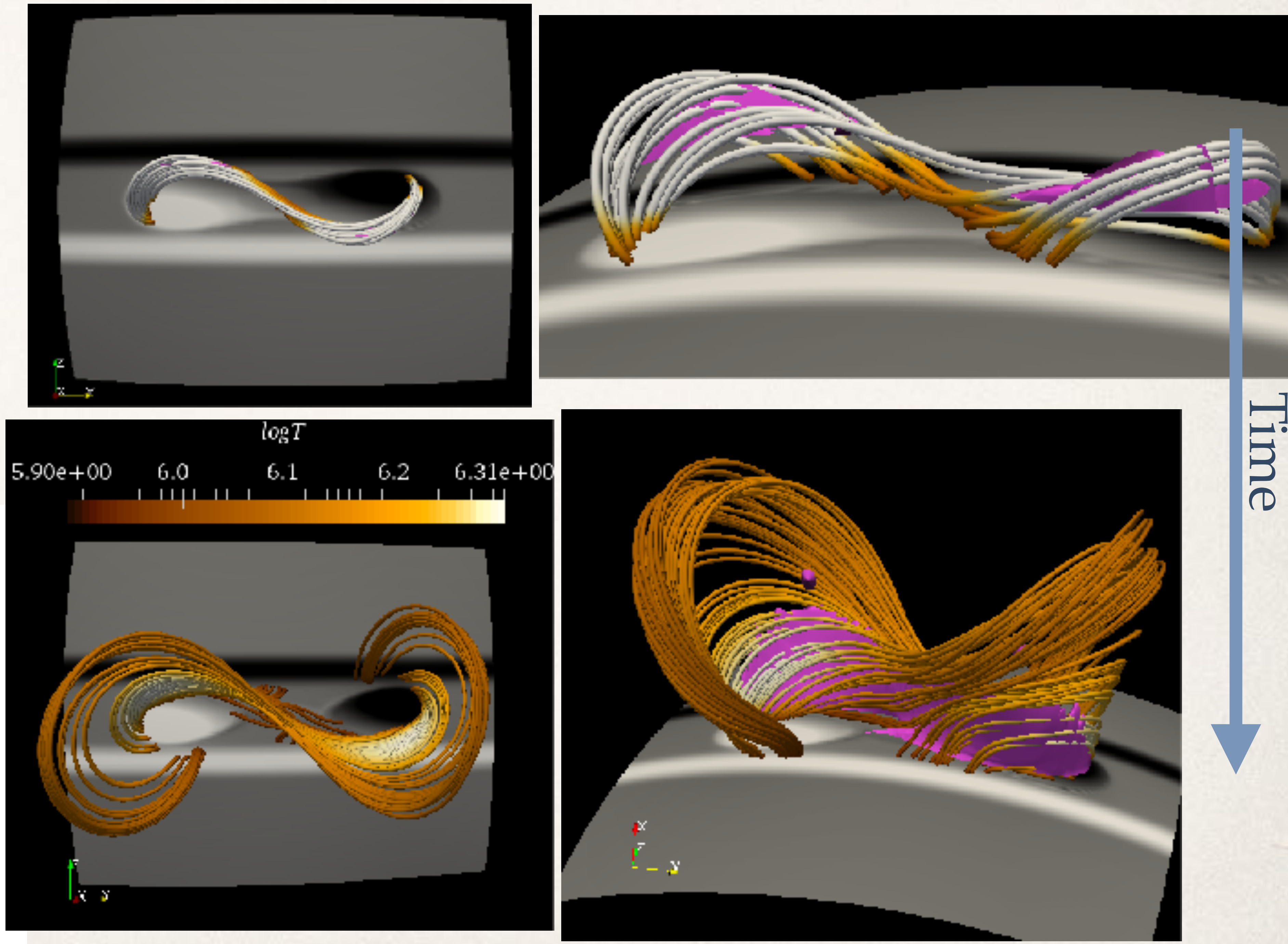

Pre-eruption coronal cavity: *Lollipop on a stick!*

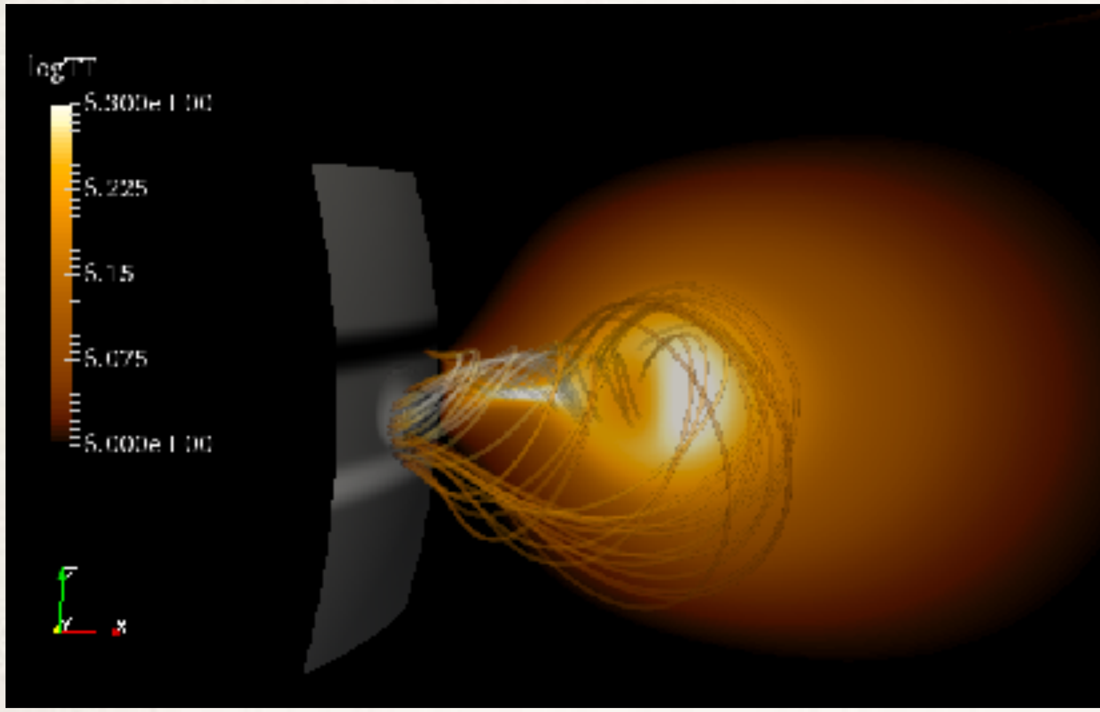

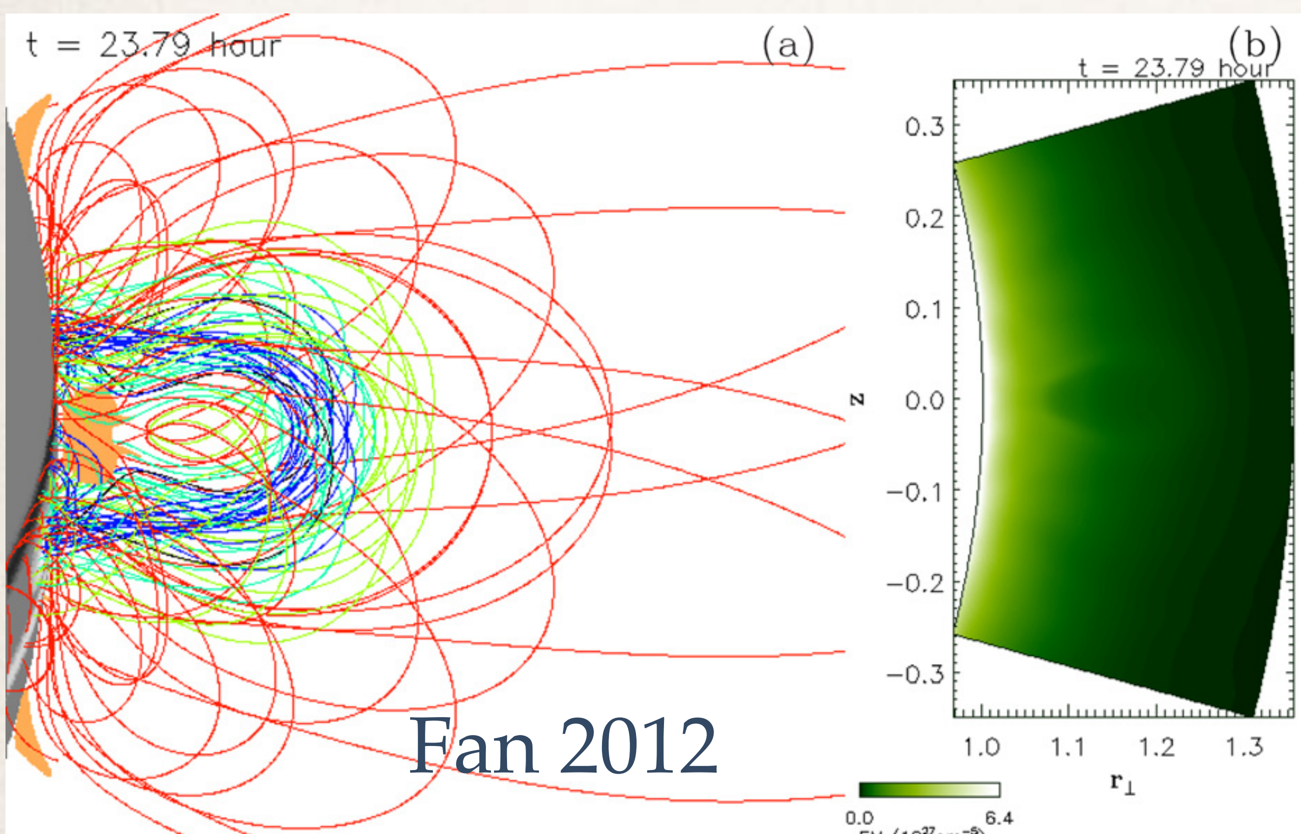

Prominence cavity SDO/AIA **[negative images]** on 13 June 2010 on NW limb (Regnier et. al. 2011)

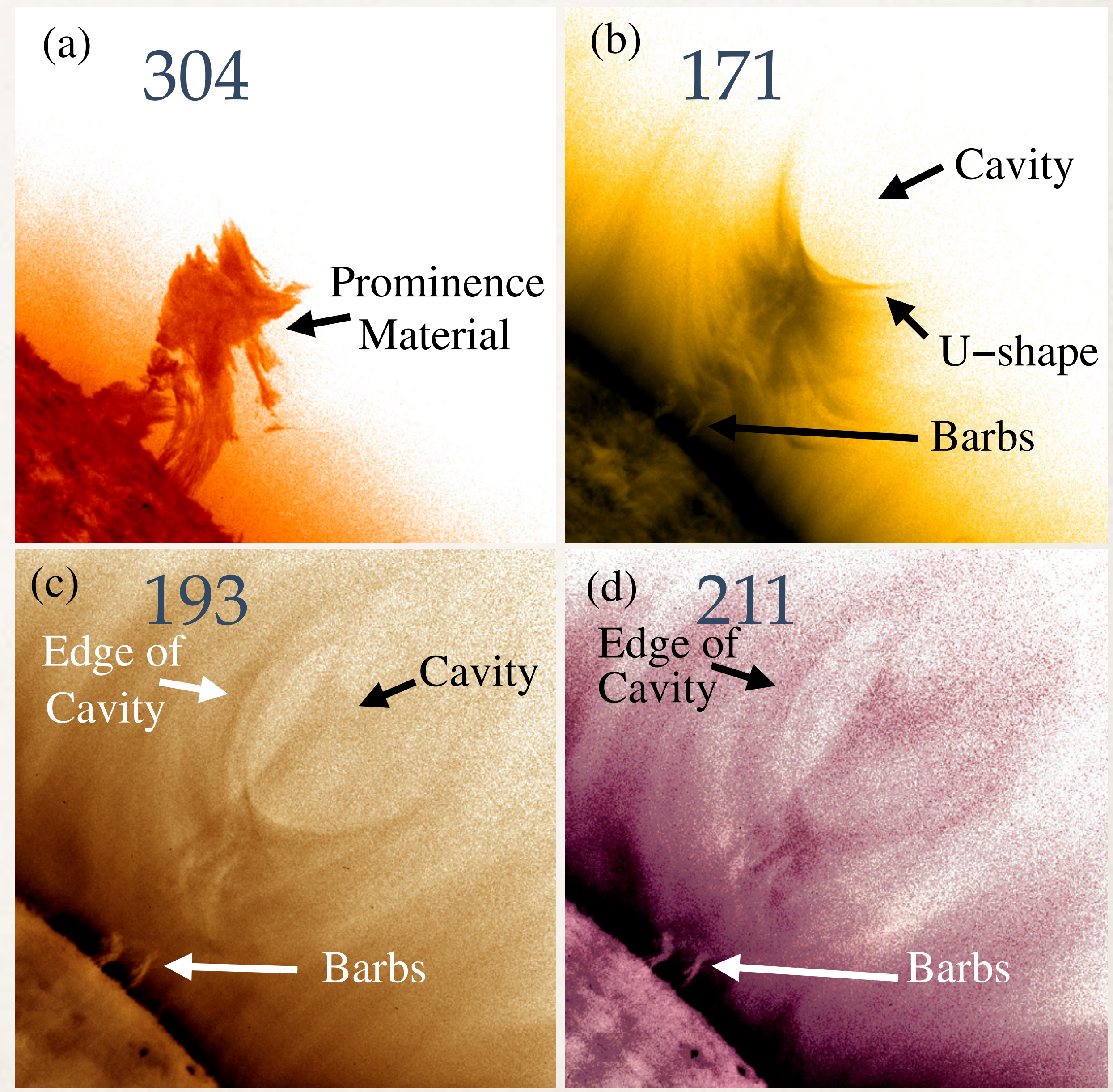

Pre-eruption coronal cavity: *Bunny ears*

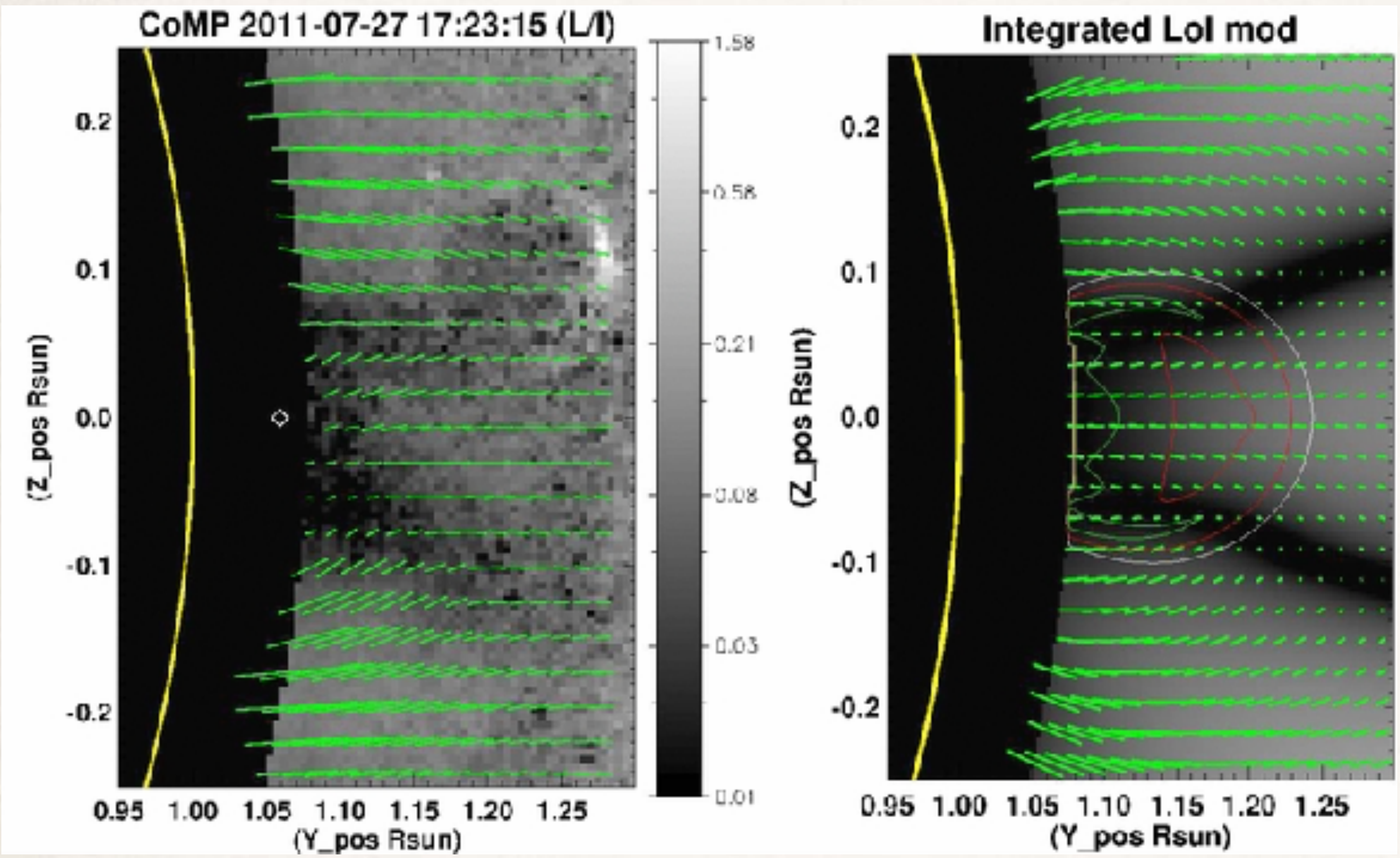

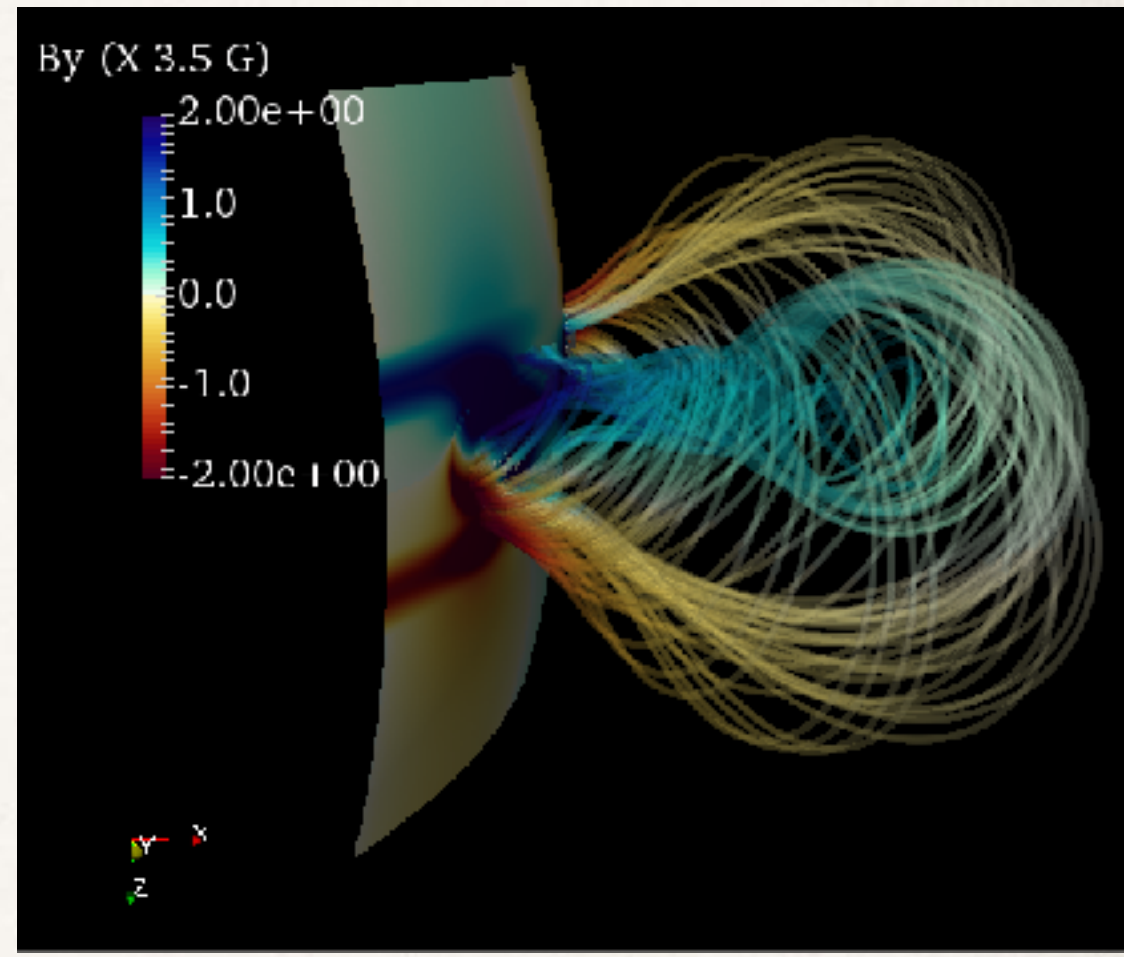

Null patterns in Stokes L/I in a Polar crown cavity
(Bak-Steślicka et. al. 2013)

$$L = \sqrt{Q^2 + U^2} \propto \sin^2 \theta$$

Supporting a prominence

1. **Mass supply:** pressure gradient due to formation of hot current channel

$$\boldsymbol{q}_s = -\kappa_0 T^{5/2} \hat{\boldsymbol{b}}\hat{\boldsymbol{b}} \cdot \nabla T,$$

Increase in Gas pressure at Chromosphere

Plasma sucked out of chromosphere

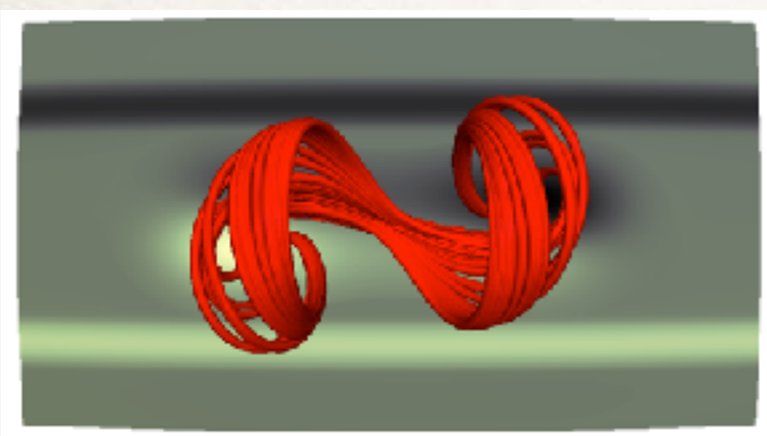

$$\left| \frac{(B \cdot \nabla)B}{\mu_0} \right| > \rho g?$$

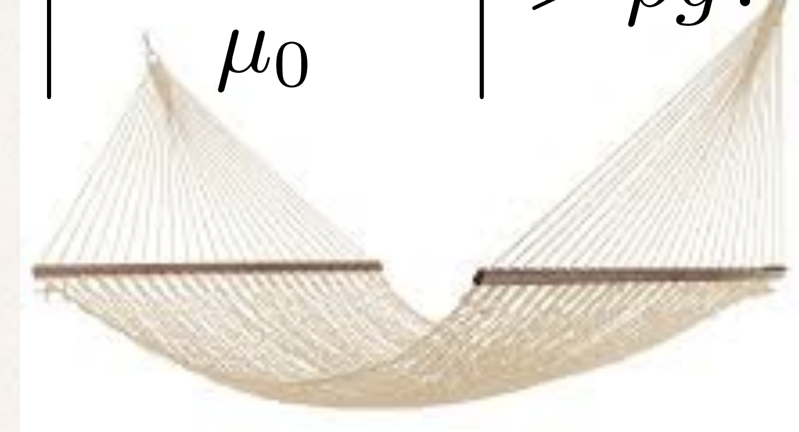

2. **Formation**: Prominence condensation due to thermal instability

Parker (1953), Field (1965)

$$\frac{\partial e}{\partial t} + \nabla \cdot (e\vec{u}) = \mathcal{H}eating - \rho^2 \Lambda(T) + \text{Others}$$

Condensed plasma falls into preexisting dips

Supporting a prominence

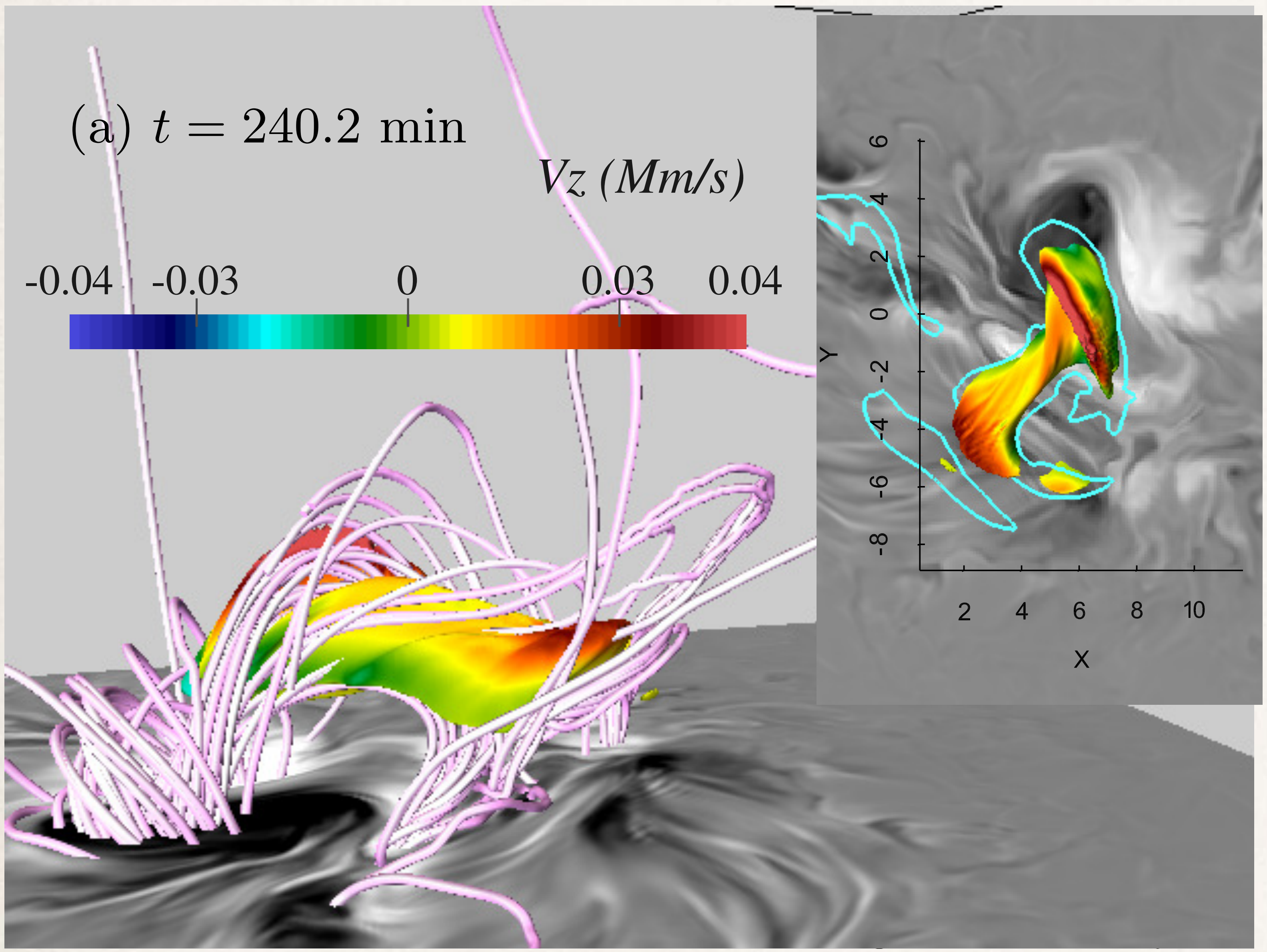

2. **Formation:** Field lines dip under the weight of the plasma. Depends on magnetic tension vs gravity

Estimated mass inside the iso-surface ~ 1.2 X 10^{13} kg
PC et. al. 2016

Typical Observed CME mass ~ 10^{11} to $4X10^{13}$ kg

3. **Destruction:** Evaporation, Rayleigh Taylor Instability, Coronal Rain

Tether cutting: Fast Release phase

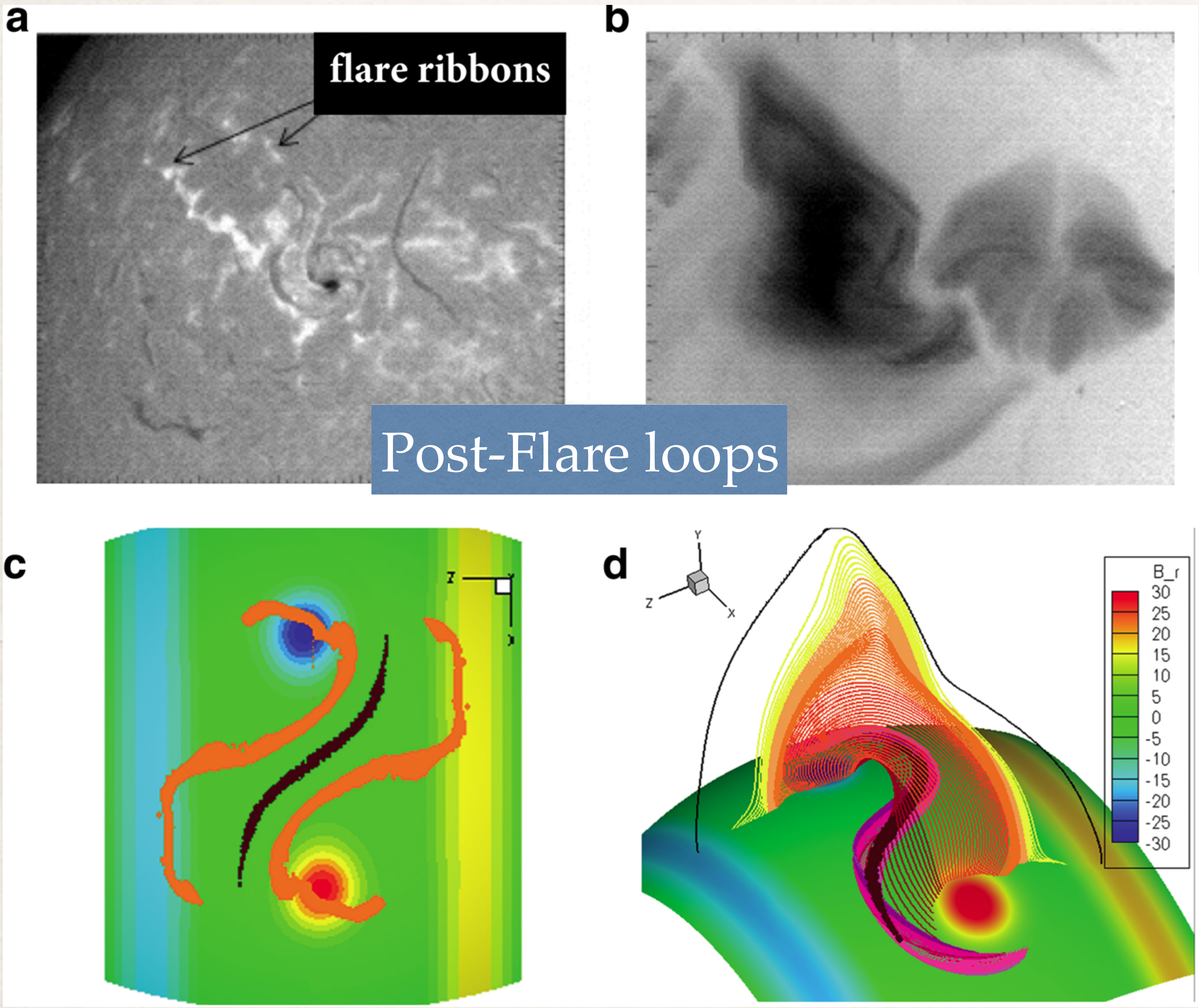

Two-Ribbon flare with foot points moving apart with time
Gibson, 2018 (LRSP)

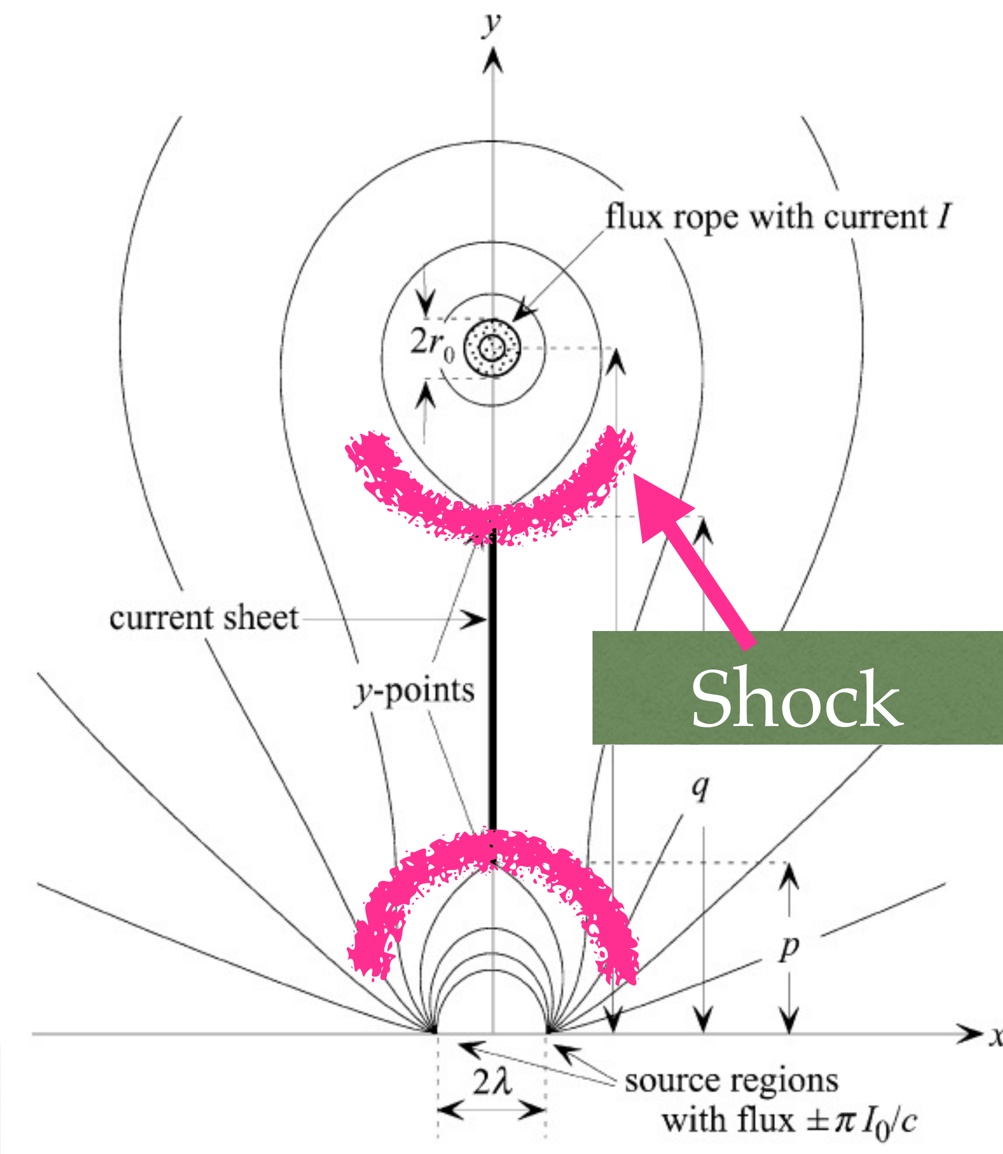

Homologous eruptions: Full MHD simulation

1. Sequence of **four homologous eruptions initiated** due to helical kink instability.

2. Flux rope **reforms** after every eruption

3. **Second** in the series is **cannibalistic**

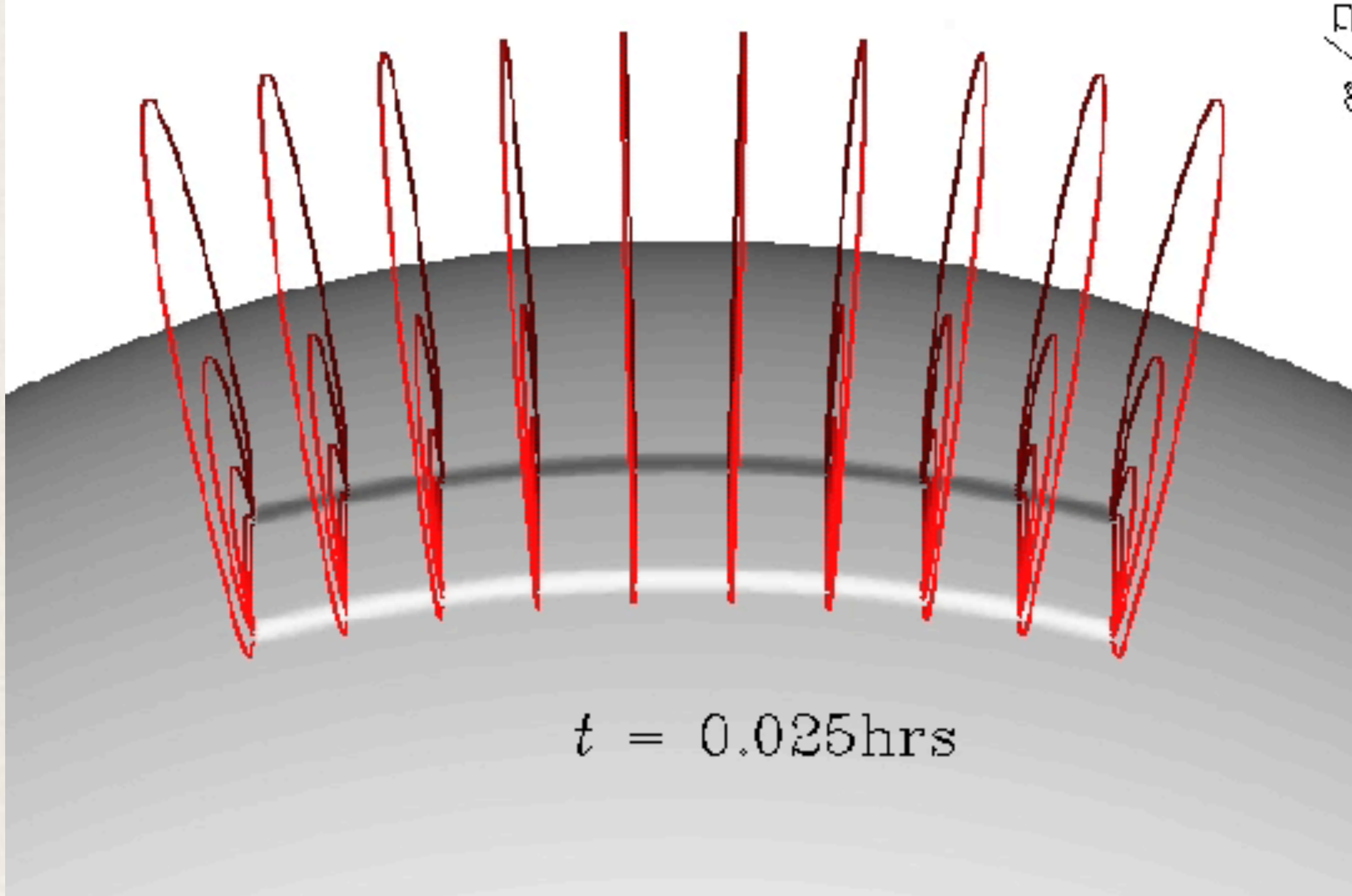

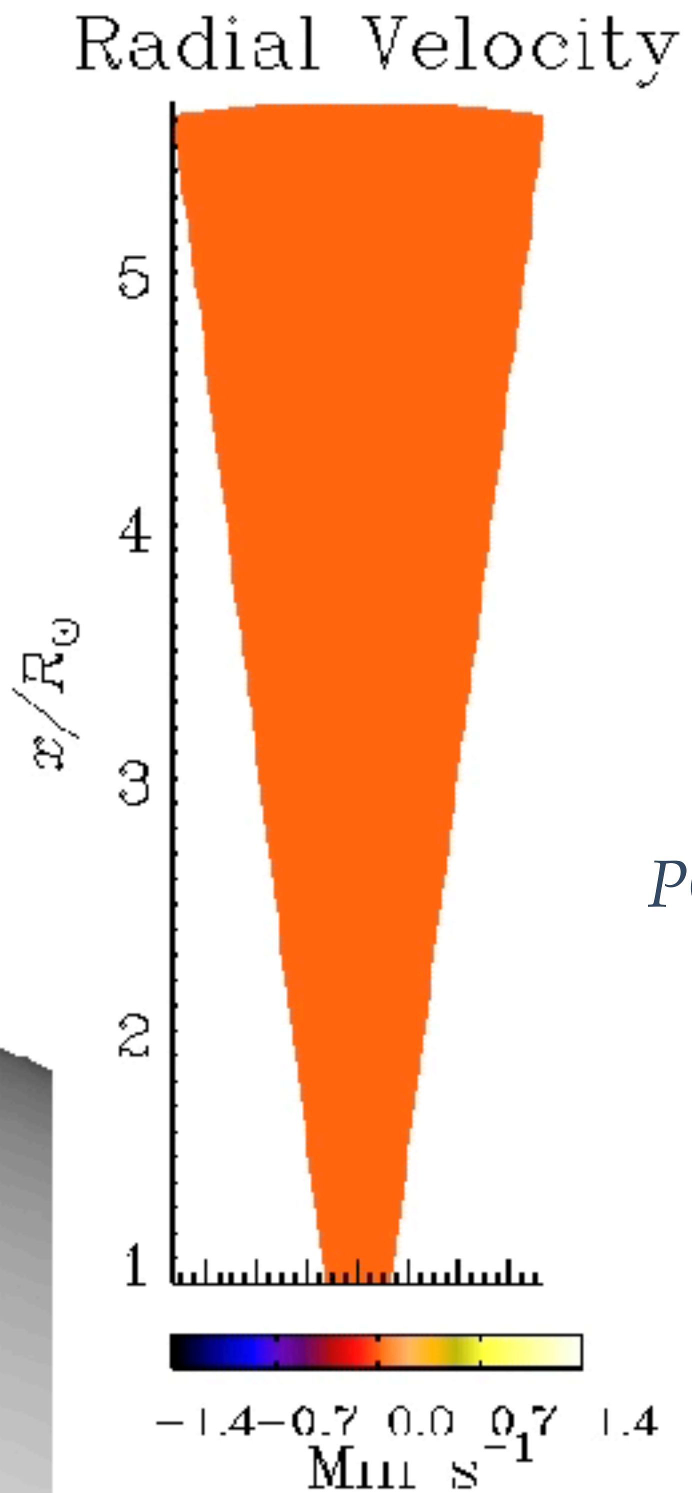

PC & Fan 2013

Height time curves for erupting flux ropes

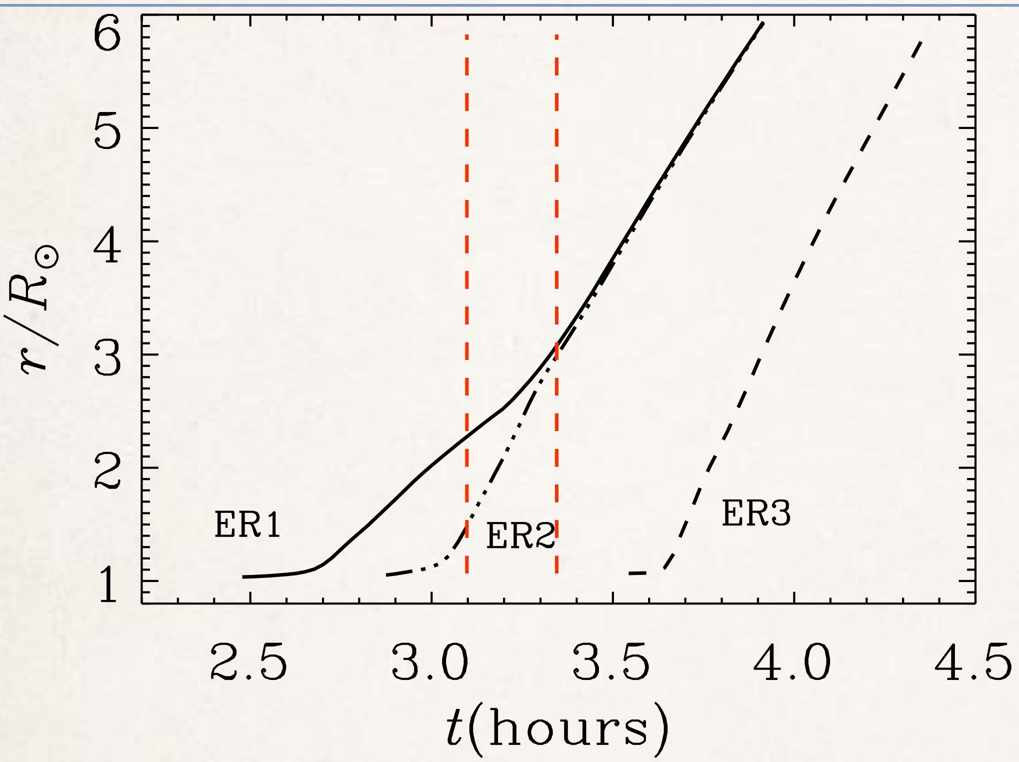

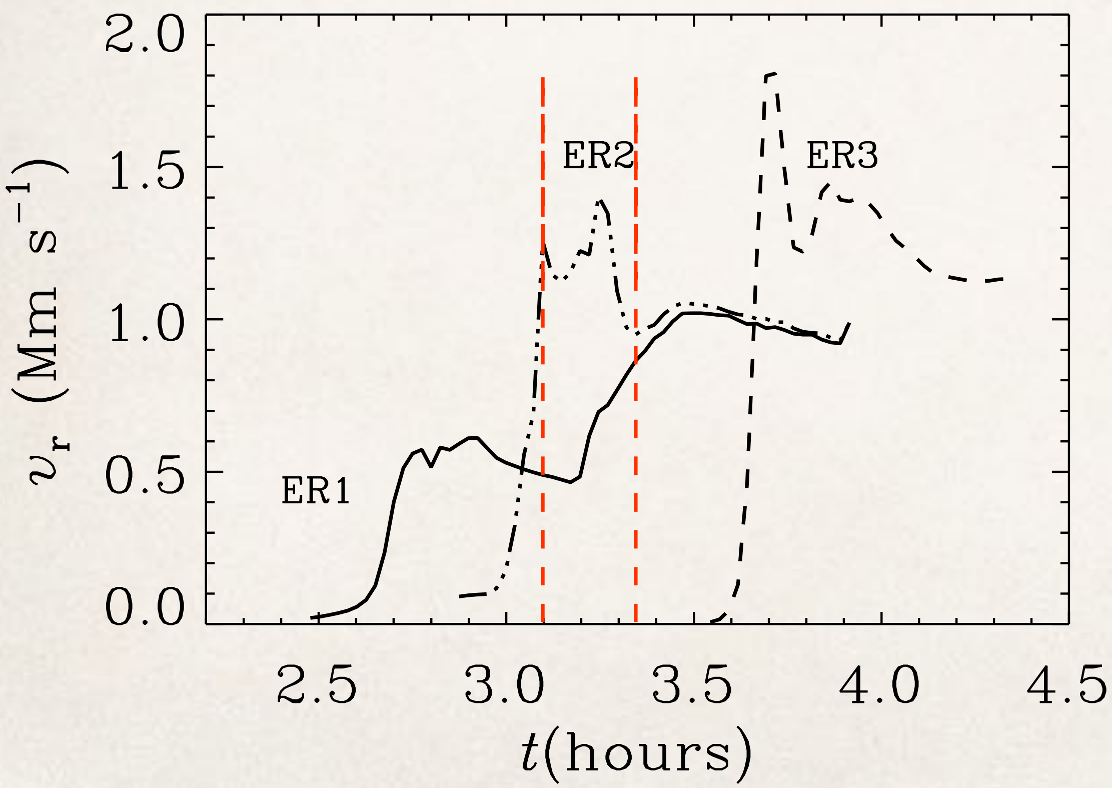

PC & Fan 2013

CME speeds :
650 km/s, 1400 km/s, 1800 km/s

Slowest CME acceleration ~ 1.6 km s^{-2}

Height at which CME acceleration initiated ~ 1.035 R_s

$$-\frac{d\ln B_{\text{pot}}}{d\ln r} \approx 1.0, 1.05, 1.1 < n_{\text{crit}} = 1.5$$

At the point of initiation all CMEs stable to TI

The twist of the field lines near the axis ~ 2.1 winds between the anchored footpoints.

Energetics of homologous eruptions

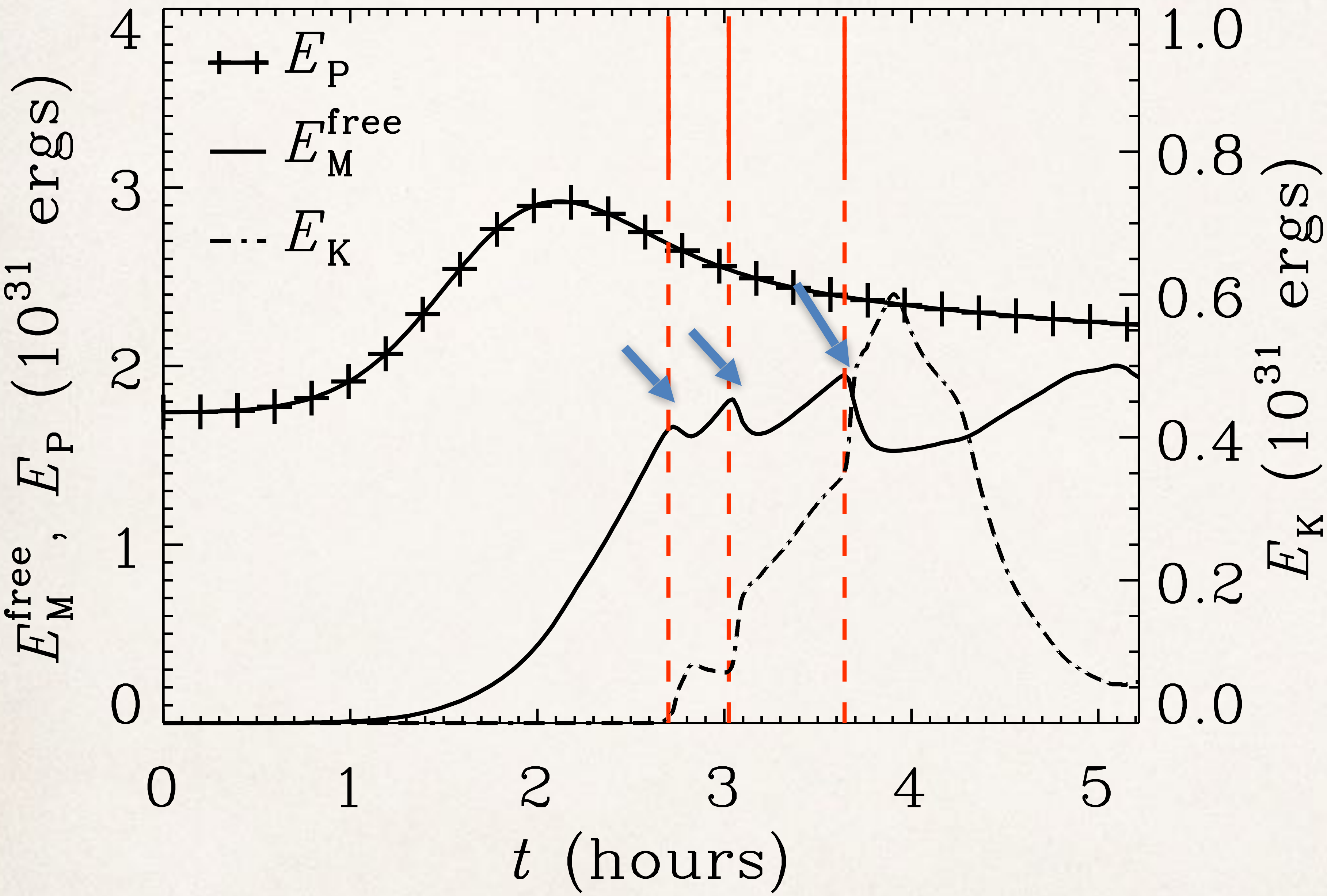

1. More magnetic free energy (MFE) available for conversion to kinetic energy (KE) for successive CMEs

2. Each CME releases the free energy only partially

PC & Fan 2013

Partial eruption: sigmoid-under-cusp

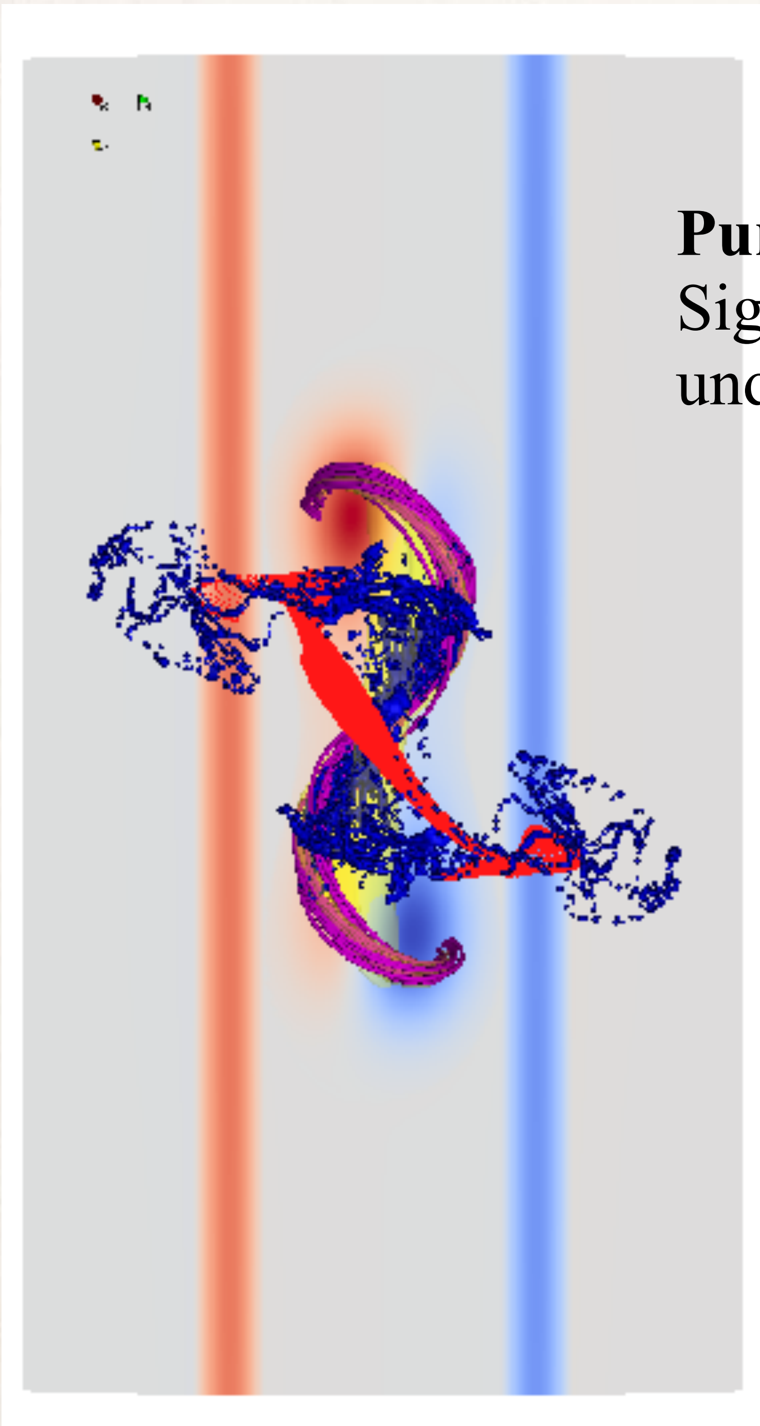

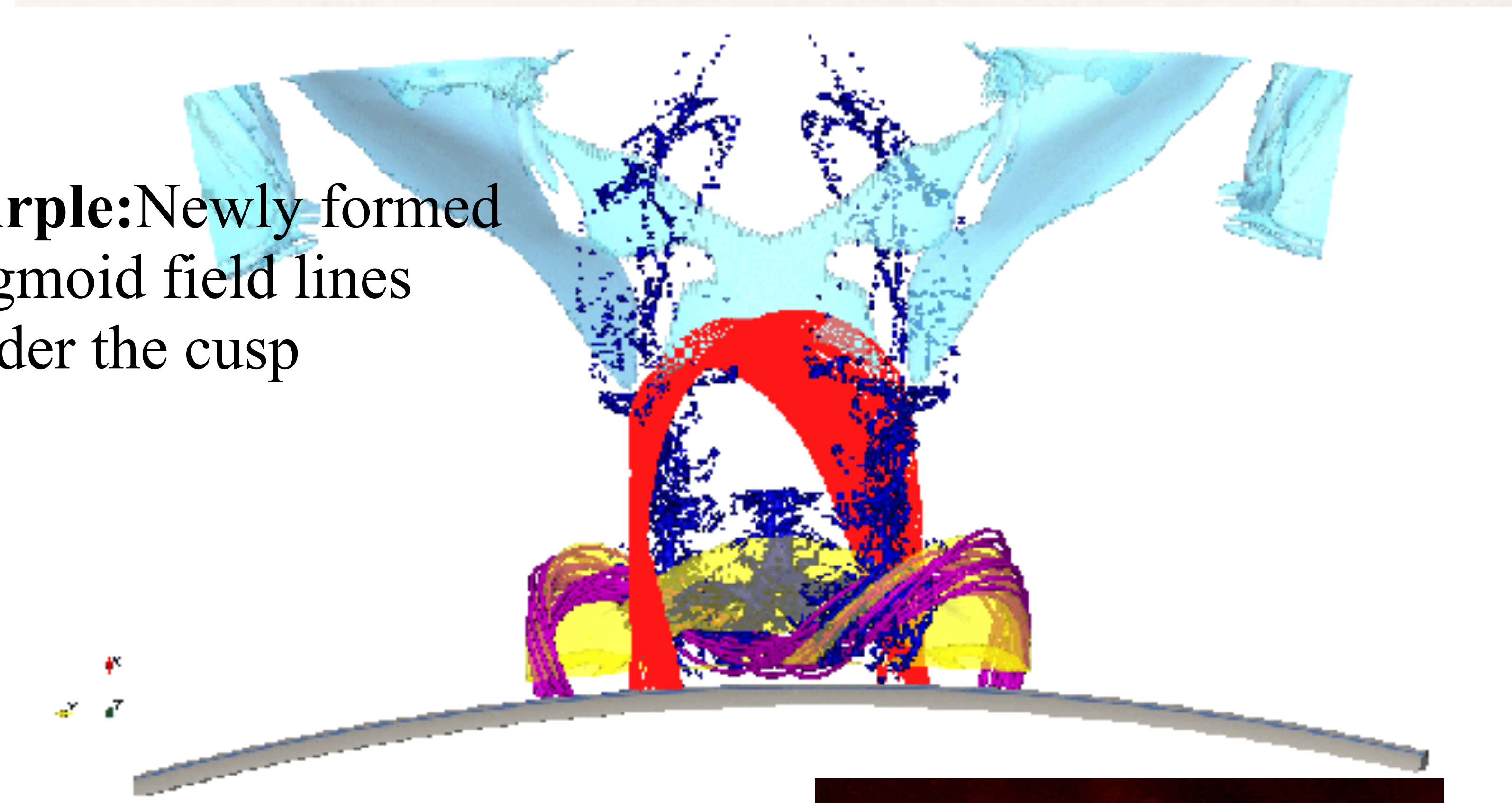

Purple: Newly formed Sigmoid field lines under the cusp

Red: Post Flare loops are reconnected field-lines formed at the bottom of an intense current sheet and are very hot ~10MK

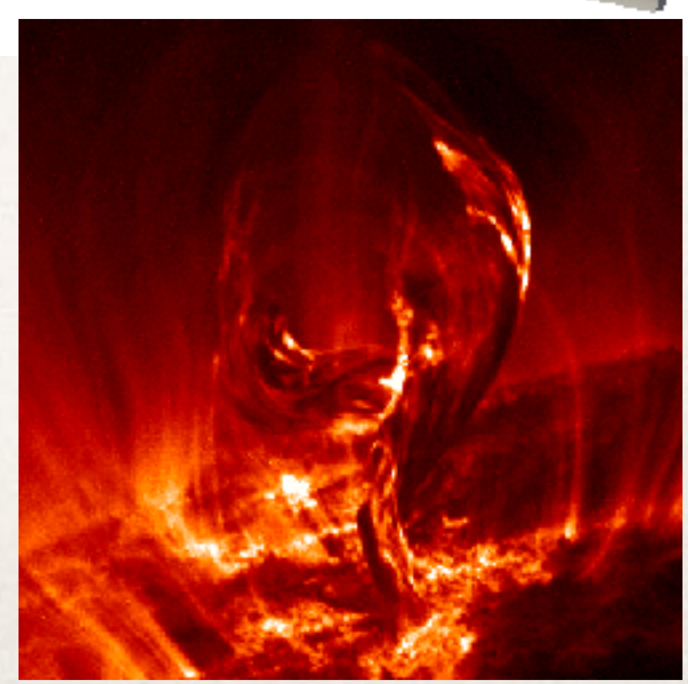

Structure of CME far from the sun

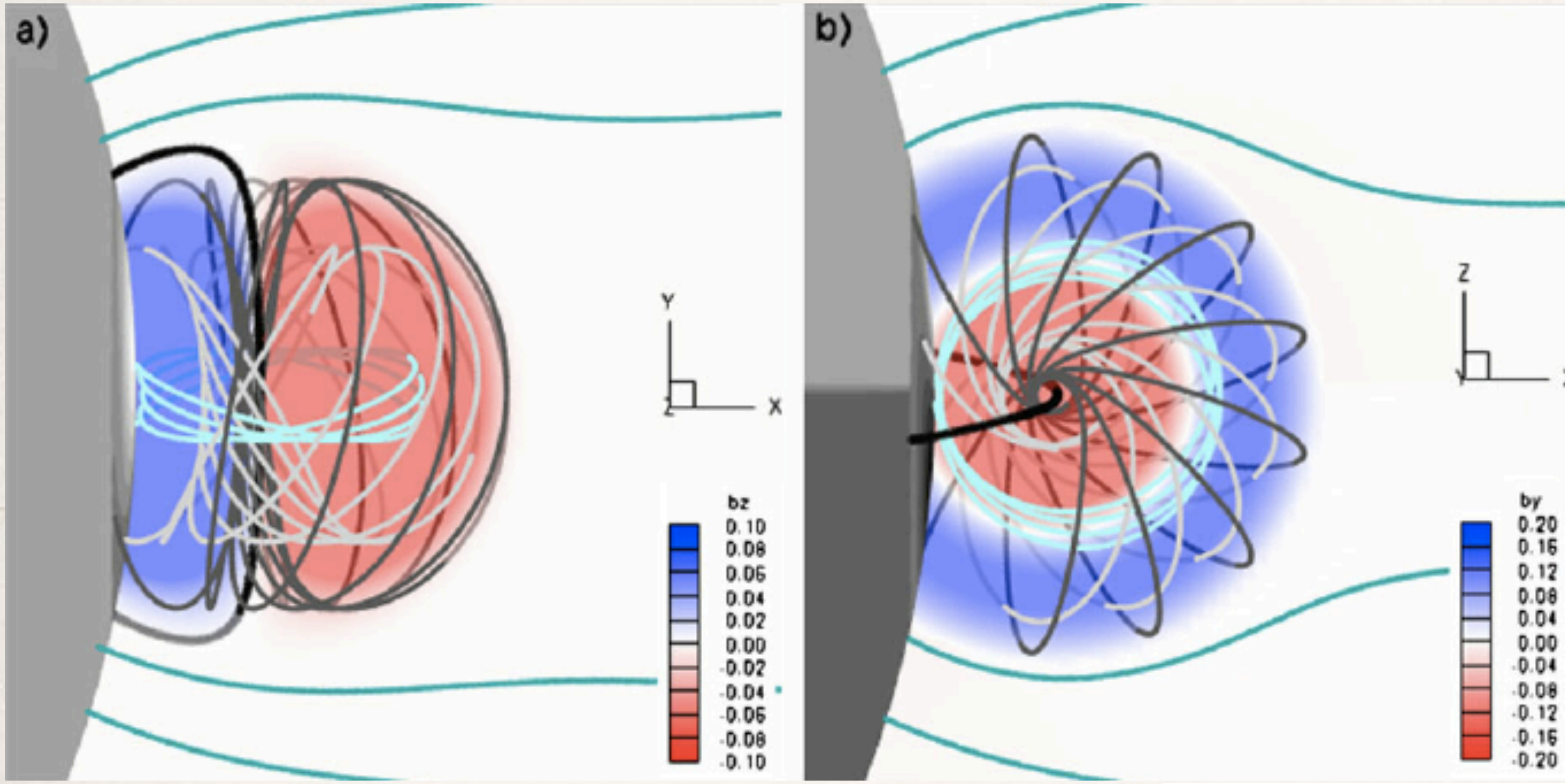

Gibson & Low (1998)
Flux rope

Spheromak

Chatterjee & Fan 2013 model